Progress In Electromagnetics Research C, Vol. 58, 117–123, 2015

Compact Tri-Band Bandpass Filter Based on Hybrid Resonator with Improved Selectivity Performances

Shuai Yang[1, *], Jian-Zhong Chen[2], Bian Wu[1], and Chang-Hong Liang[1]

Abstract—A novel microstrip tri-band bandpass filter is proposed and implemented using hybrid resonator with independently controllable center frequencies and good in-between isolation. This hybrid resonator is constructed by a stepped-impedance stub resonator and a single end shorted resonator. The stepped-impedance stub resonators are applied to achieve the first and second passband, while the third passband is implemented by single end shorted resonators. By applying the even-odd mode approach, the resonance frequency ratio between even mode and odd mode inside the stepped-impedance stub resonators is attained. Furthermore, the filter with multi-path coupling structure can generate the transmission zeros at the edge of the passband, which can effectively improve the filter passband selectivity. Finally, a tri-band filter operating at 1.91, 2.73, and 3.45 GHz is designed and fabricated. The measurement results accord well with the full-wave electromagnetic designed responses.

1. INTRODUCTION

With the rapid development of multiple bands operation for wireless communication applications, tri-band bandpass filters (BPFs) have gained a lot of attention of many researchers in recent years. Various design approaches and structures have been used to develop tri-band BPFs. Classical resonators include stub-loaded resonators (SLRs), and stepped-impedance resonators (SIRs) were widely used to design tri-band BPFs [1–10]. Modified stub-loaded resonator [1–4] was utilized to design tri-band BPFs. A series of multi-stub loaded resonators were used to design tri-band BPFs [1, 2]. In the analysis of multi-stub loaded resonator, even- and odd-mode analysis is utilized twice to analyze its resonance characteristics. In [3], a tri-band filter was designed by one set of stub-loaded short-ended resonators. Three embedded bending stub resonators were employed to achieve tri-band filter with compact size [4]. Other typical methods were utilized to modified forms of stepped-impedance resonators (SIRs) in [5–10]. A multimode stepped-impedance resonator with a 0° tapped-feed structure was proposed to design a miniaturized tri-band BPF in [5]. To provide more freedom to control the filter harmonics responses, tri-section stepped-impedance resonators (TSSIRs) were proposed to build up tri-band BPFs [6, 7]. Moreover, a tri-band BPF based on two modified TSSIRs was present in [8]. In [9], a compact tri-band BPF using multipath-embedded resonators (MERs) was proposed, which consisted of two centrally connected the SIRs. In [10], two direct-coupled stepped impedance resonators (SIRs) with open stubs were proposed to design a compact tri-band BPF.

Besides these classical resonators, some novel resonators were also widely used, such as modified forms of stepped-impedance resonators (SIRs) [11–14], ring resonators [15, 16], and assembled resonators [17, 18]. In [11], open stub-loaded shorted stepped-impedance resonator (OSLSSIR), which consisted of a two-end-shorted TSSIR with two identical open stubs loaded at its impedance junctions,

Received 18 May 2015, Accepted 6 July 2015, Scheduled 14 July 2015

* Corresponding author: Shuai Yang (shyangxidian@gmail.com).

[1] National Laboratory of Science and Technology on Antennas and Microwaves, Collaborative Innovation Center of Information Sensing and Understanding at Xidian University, Xi'an, Shaanxi 710071, P. R. China. [2] School of Electronic and Information Engineering, Xi'an Jiaotong University, Xi'an, Shaanxi 710049, P. R. China.

was used to design a tri-band BPF. Moreover, a compact tri-band BPF using open stub loaded tri-mode $\lambda/4$ SIR with excellent band-to-band isolation was presented in [12]. Also, a pair of asymmetric SIRs with parallel coupling arrangement was proposed to perform the tri-band responses in [13, 14]. A ring resonator with three pairs of degenerate modes was utilized for tri-band operation by controlling the perturbations of four open stubs [15]. Furthermore, improved configurations with dual-mode double-square-loop resonators (DMDSLRs) for tri-band filter were presented in [16]. Other design modes of tri-band BPF which combined two kind resonators is proposed in [17, 18]. In [17], a tri-band filter was proposed where the DGS-based resonators resulted in the first passband, and stub-loaded resonators contributed to the second and third band. In [18], the assembled resonators constructed by a SIR and a common half-wavelength resonators were proposed to achieve the tri-band BPF.

In this paper, a compact tri-band BPF based on hybrid resonator which consists of stepped-impedance stub resonators (SISRs) and single end shorted resonators (SESRs) is presented. The resonant behavior of SISRs and SESRs is analyzed in detail firstly, then multi-path coupling structure of the proposed filter is investigated thoroughly. After a study on the mechanism of hybrid resonator, a tri-band BPF is designed and fabricated to provide an experimental verification on the proposed filter.

2. DESIGN AND ANALYSIS OF THE TRI-BAND BANDPASS FILTER

Figure 1 illustrates the layout of the proposed tri-band BPF based on hybrid resonator. It consists of stepped-impedance stub resonators (SISRs) and single end shorted resonators (SESRs). The stepped impedance stub of SISRs is bent upward, while the SESRs are embeded inside the SISRs to achieve the tri-band BPF. To miniaturize the overall size, all the stubs of SISR and SESR employ a bending structure. Multi-path coupling structure is achieved by stub-to-stub coupling of SISRs and SESRs. On the other hand, outer resonators SISRs operate at the first and second passband frequencies, i.e., f_1 and f_2. And the SESRs operate at the third passband frequency f_3.

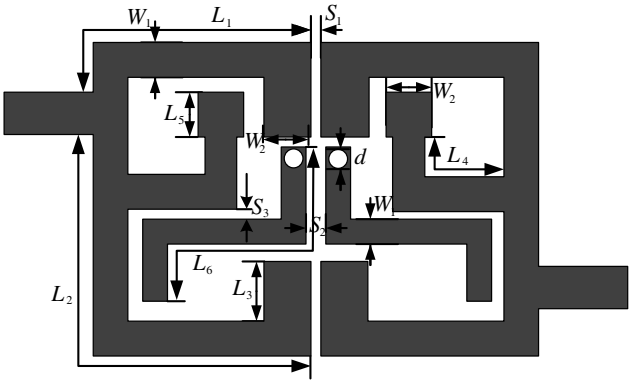

Figure 1. Physical layout of the proposed tri-band BPF based on hybrid resonator.

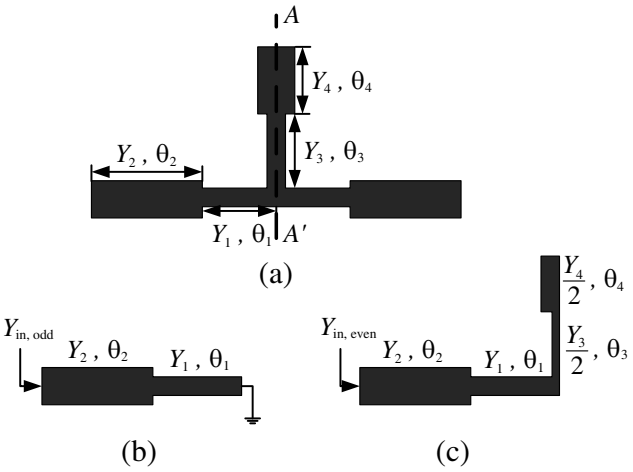

Figure 2. (a) Original structure of SISRs. (b) Odd-mode equivalent circuit of SISRs. (c) Even-mode equivalent circuit of SISRs.

2.1. Resonant Behavior Analysis of Hybrid Resonator

Figure 2 shows the equivalent circuit of the SISRs. Since the presented SISRs are symmetrical in structure, the even- and odd-mode approach can be applied to analyze it. The voltage is null along the plane A-A' when odd-mode excitation is applied, which results in the odd-mode equivalent circuit of Figure 2(b). The input admittance for odd-mode can be derived as

$$Y_{\text{in,odd}} = jY_2 \frac{Y_2 \tan\theta_2 - Y_1 \cot\theta_1}{Y_2 + Y_1 \tan\theta_2 \cot\theta_1} \tag{1}$$

For the even-mode excitation, the equivalent circuit is shown in Figure 2(c). Under the special case of $2Y_2 = Y_4$, $2Y_1 = Y_3$, and $\theta_2 = \theta_4$, the input admittance of even mode is expressed as

$$Y_{\text{in,even}} = jY_2 \frac{2\left(K\tan\left[(\theta_1+\theta_3)/2\right]+\tan\theta_2\right)\left(K-\tan\left[(\theta_1+\theta_3)/2\right]\tan\theta_2\right)}{K\left(1-\tan^2\theta_2\right)\left(1-\tan^2\left[(\theta_1+\theta_3)/2\right]\right)-2\left(1-K^2\right)\tan\left[(\theta_1+\theta_3)/2\right]\tan\theta_2} \tag{2}$$

where the $\theta_i = \beta \cdot l_i$ (i = 1, 2, 3) is the electric length of the microstrip line, Y_i (i = 1, 2, 3, 4) the characteristic admittance of the microstrip line, and $K = Y_2/Y_1$ the admittance ratio of high- and low-admittance lines.

In order to simplify the analysis, $\theta_1 = 2\theta_2$, $\theta_3 = \theta_1$ are assumed in the derivation. From the resonance condition of $Y_{\text{in,odd}} = 0$, and $Y_{\text{in,even}} = 0$, the first five resonance frequencies of SISR can be obtained from (1) and (2),

$$f_{\text{odd}} = \left(\frac{c}{2\pi L_2}\right)\tan^{-1}\sqrt{\frac{K}{2+K}} \tag{3a}$$

$$f_{\text{even1}} = \left(\frac{c}{2\pi L_2}\right)\tan^{-1}\sqrt{\frac{K}{2+K}} \tag{3b}$$

$$f_{\text{even2}} = \left(\frac{c}{2\pi L_2}\right)\tan^{-1}\sqrt{\frac{(K+2)}{K}} \tag{3c}$$

$$f_{\text{even3}} = \frac{c}{4L_2} \tag{3d}$$

$$f_{\text{even4}} = \frac{c}{2L_2} \tag{3e}$$

Since the first even-mode frequency is equal to the odd-mode frequency, normalized frequency ratios are summarized

$$\frac{f_{\text{even2}}}{f_{\text{odd}}} = \frac{\tan^{-1}\sqrt{\frac{K+2}{K}}}{\tan^{-1}\sqrt{\frac{K}{2+K}}} \tag{4a}$$

$$\frac{f_{\text{even3}}}{f_{\text{odd}}} = \frac{\pi}{2\tan^{-1}\sqrt{\frac{K}{2+K}}} \tag{4b}$$

$$\frac{f_{\text{even4}}}{f_{\text{odd}}} = \frac{\pi}{\tan^{-1}\sqrt{\frac{K}{2+K}}} \tag{4c}$$

In order to further analyze the resonant characteristics, the design graph of admittance ratio (K) and frequency ratio ($f_{\text{even}i}/f_{\text{odd}}$, i = 1, 2, 3, 4) are shown in Figure 3. It can be observed that by decreasing the value of K ($K < 1$), the even-mode frequency deviates away from the fundamental frequency. This feature is useful for achieving multi-band BPFs. However, for $K > 1$, the even-mode frequency is close to the fundamental frequency so that the wideband filter can be achieved. In order to design the tri-band BPF, admittance ratio K is set at 0.7. The first even-mode frequency is equal to the odd-mode frequency; the even-mode frequencies of f_{even2} and f_{even3} are always close to each other, which make up the second bandpass, while the even-mode frequency of f_{even4} is far away the other even-mode frequency. As a consequence, the third bandpass is designed by introducing the SESRs.

The $\lambda/4$ single-end shorted resonators (SESRs) are introduced to make up the tri-band BPF with the SISRs. Figure 4 illustrates the configuration of the $\lambda/4$ single end shorted resonators. The total length L of the $\lambda/4$ SESRs is approximately determined by the following equation:

$$L = \frac{c}{4f\sqrt{\varepsilon_{eff}}} \tag{5}$$

where f is the resonance frequency, c the light speed in free space, and ε_{eff} the effective dielectric constant of the substrate. Therefore, the third bandpass frequency is mainly determined by the length of the SESRs, and proper selection of the coupling dimensions can obtain desired bandpass performance.

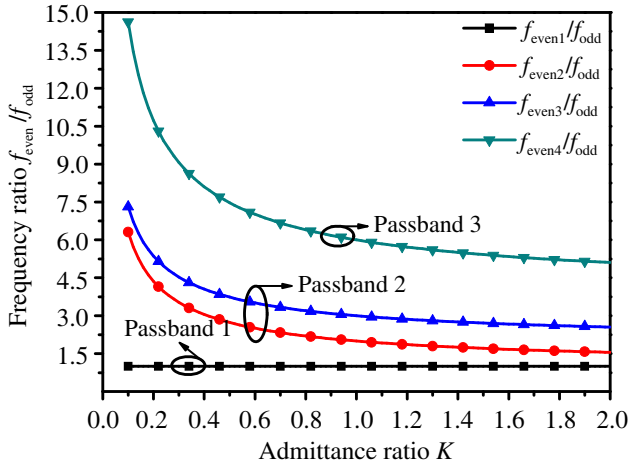

Figure 3. The design graph of the normalized f_2/f_1 and admittance ratio K.

Figure 4. Layout of single end short circuited resonator.

2.2. Analysis of Characteristics Coupling

To achieve the desired bandwidth for the three passbands, adjusting the coupling dimensions of the proposed filter is necessary. The first bandpass is formed by splitting the first even-mode and odd-mode frequencies, due to the introduction of the stub-to-stub coupled structure [19].

On the other hand, the coupling coefficients related with the desired fractional bandwidths is controlled by the coupling spacing S_1, S_2, and S_3 between the SESRs and SISRs. The external quality factor (Q_e) at the corresponded resonant frequencies with respect to the length t defined by the tapped location to the symmetric plane is analyzed. The coupling coefficients ($K_{i,j}$) and external quality factor (Q_e) can be calculated from full-wave simulated transmitted coefficients, expressed as [20]

$$k_{i,j} = \frac{f_{p2}^2 - f_{p1}^2}{f_{p2}^2 + f_{p1}^2} \tag{6}$$

$$Q_e = \frac{2\omega_0}{\Delta\omega_{3\,\mathrm{dB}}} \tag{7}$$

where f_{p2} and f_{p1} are defined to be the higher and lower of the two resonant modes. ω_0 is the resonant frequency and $\Delta\omega_{3\,\mathrm{dB}}$ the bandwidth for which the attenuation for S_{21} is up 3 dB from that at resonance. To satisfy the desired coupling coefficients, the coupling spacing (S_1, S_2, and S_3) can be determined as 0.4, 1.25, 0.3 mm. The external quality factors (Q_e) are calculated by full-wave EM simulation shown in Figure 5. It is easily found that the designed external quality factors (Q_e) are dependent on the tapped location t. The desired tri-band response can be obtained simultaneously by shifting t to induce a suitable the Q_e for the bandwidths, where t is chosen to be 4.525 mm.

Figure 6 shows the multi-path coupling structure of the proposed filter. The solid lines represent the direct coupling routes. Resonators A and B in this figure represent the SISR and SESR, and the superscripts e and o of the SISR denote the even and odd resonant modes, respectively. It is seen from Figure 6 that there are three parallel coupling routes between the input and output. Resonator A^o operates at the first passband, and resonator A^e operates at the third passband, which is based on even- and odd-mode analysis. Besides, in RF passage 2, resonator B realizes bandpass response combined with SISRs. As a consequence, a tri-band BPF is achieved by the proposed coupling structure, which may introduce transmission zeros in the insertion loss response.

The external couplings of the three passages are accomplished by the 0° feed structure, which can improve the selectivity performance of proposed tri-band BPF [21].

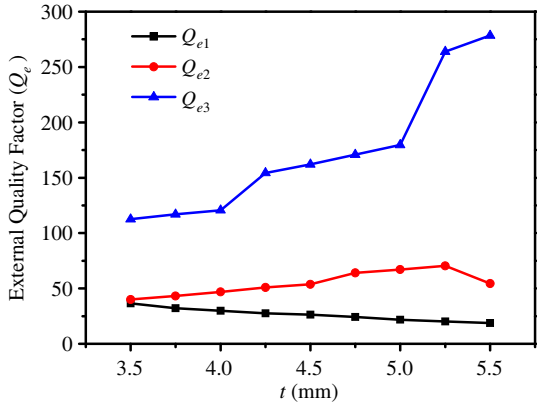

Figure 5. External quality factors of three passbands respect to tapped location of t.

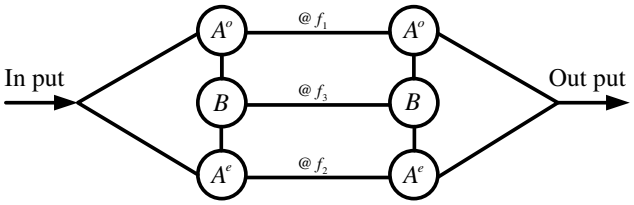

Figure 6. Multi-path coupling structure of the proposed filter.

3. EXPERIMENTAL VERIFICATION AND RESULT

Based on the detailed discussion in the above section, a tri-band filter is designed and fabricated on a substrate with a dielectric constant $\varepsilon_r = 2.65$, loss tangent $\tan\delta = 10^{-3}$ and a thickness of $h = 1$ mm. After an optimal design process, the final dimensions of the proposed structure are given in Table 1.

A photograph of the fabricated BPF is shown in Figure 7. The overall physical circuit size of the fabricated tri-band BPF is $0.14\lambda_g \times 0.13\lambda_g$, where λ_g is the guided wavelength at the center frequency of first passband frequency. Figure 8 illustrates the simulated and measured responses, accomplished by using IE3D and Agilent 8719ES network analyzer, respectively. A good agreement is observed between the simulation and measurement over the plotted frequency range. The measured triple passbands are

Table 1. Physical parameters of the filter (all in mm).

Parameter	W_1	W_2	L_1	L_2	L_3	L_4
Value	1.2	2.2	24.2	15.1	6.1	7.5
Parameter	L_5	L_6	S_1	S_2	S_3	d
Value	3.9	16.5	0.4	1.25	0.3	0.8

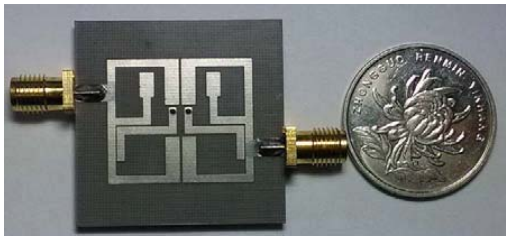

Figure 7. Photograph of the fabricated BPF.

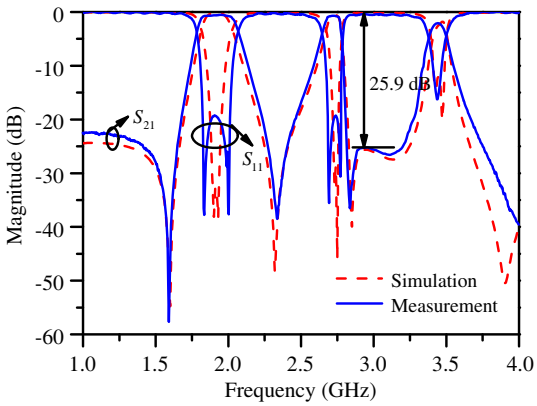

Figure 8. Simulated and measured results of the proposed tri-band BPF.

centered at 1.91, 2.73, and 3.45 GHz with the 3-dB fractional bandwidths of 10.6%, 3.86%, and 3.45%, respectively, as can be found from Figure 8. The measured insertion losses (IL) including the loss from SMA connectors are 0.51, 0.69, and 1.15 dB, and the return losses (RL) within the three passbands are 18.5, 18.7, and 25 dB, respectively.

In addition, the proposed tri-band BPF generates four transmission zeros at 1.58, 2.32, 2.85, and 3.9 GHz, thus significantly improving the band-to-band isolation among these passband. In particular, the rejection level between the second and third passbands is 25.21 dB. Finally, Table 2 is tabulated and provided to compare the proposed tri-band filter with other reported tri-band BPF in [3, 8, 17], and [18] in terms of key parameters. It can be observed that the proposed filter has the advantages of low insertion loss, high band-to-band isolation level and compact size.

Table 2. Comparisons of the proposed filter with other reported tri-band filter.

Ref.	Ref. [3]	Ref. [8]	Ref. [17]	Ref. [18]	Proposed Filter
Substrate/height (mm)	6.15/0.635	2.2/0.787	2.65/1	2.55/0.8	2.65/1
Center frequency (GHz)	1.95/3.46/5.25	2.4/3.5/5.5	2.45/3.5/5.25	2.45/3.5/5.25	1.91/2.73/3.45
IL (dB)	1.5/1.2/1.6	1.26/1.37/1.41	0.9/1.7/2.1	1.8/0.8/1.3	0.51/0.69/1.15
RL (dB)	15/20/21	13/14/10	15/20/21	17/15/12	18.5/18.7/25
Isolation (dB)	21	17	17.5	15	25.21
FBW (%)	9.7/6.4/9	N/A	12.3/6.2/3.3	2/2/3	10.6/3.86/3.45
Area (λ_g)	0.29×0.25	N/A	0.26×0.32	0.19×0.17	0.14×0.13

(λ_g is the guided wavelength at the center frequency of first passband frequency.)

4. CONCLUSIONS

In this paper, a novel compact tri-band BPF is proposed and designed based on hybrid resonator, which consists of a stepped-impedance stub resonator and single end short circuited resonator. The SISRs are designed to form the first and third passbands at 1.9 and 3.5 GHz, while the SESRs are utilized to generate the second passband at 2.7 GHz. Both the resonant and coupling properties are carefully analyzed. The tri-band filter with multi-path coupling scheme can produce transmission zeros between each two bands, and the 0° feed structure is introduced to achieve steep skirt selectivity. Based on the analysis, a tri-band BPF operated at 1.91, 2.73, and 3.45 GHz is designed, fabricated and measured. The good agreement between the simulated and measured results validates the effectiveness of the proposed tri-band BPF.

ACKNOWLEDGMENT

This work was supported by the National Natural Science Foundation of China (NSFC) under project Nos. 61271017 and 61072017.

REFERENCES

1. Gao, L., J. Xiang, and Q. Xue, "Novel compact tri-band bandpass filter using multi-stub-loaded resonator," *Progress In Electromagnetics Research C*, Vol. 50, 139–145, 2014.
2. Gao, L., X.-Y. Zhang, B.-J. Hu, and Q. Xue, "Novel multi-stub loaded resonators and their applications to various bandpass filters," *IEEE Trans. Microw. Theory and Tech.*, Vol. 62, No. 5, 1162–1172, May 2014.
3. Zhang, X. Y., L. Gao, Z. Y. Cai, and X.-L. Zhao, "Novel tri-band bandpass filter using stub-loaded short-ended resonator," *Progress In Electromagnetics Research Letters*, Vol. 40, 81–92, 2013.

4. Peng, Y., L. Zhang, Y. Leng, and J. Guan, "A compact tri-band passband filter based on three embedded bending stub resonators," *Progress In Electromagnetics Research Letters*, Vol. 37, 189–197, 2013.
5. Liu, H.-W., Y. Wang, X.-M. Wang, J.-H. Lei, and W.-Y. Xu, "Compact and High selectivity tri-band bandpass filter using multimode stepped-impedance resonator," *IEEE Microw. Wireless Compon. Lett.*, Vol. 23, No. 10, 536–538, Oct. 2013.
6. Hsu, C.-G., C.-H. Lee, and Y.-H. Hsieh, "Tri-band bandpass filter with sharp passband skirts designed using tri-section SIRs," *IEEE Microw. Wireless Compon. Lett.*, Vol. 18, No. 1, 19–21, Jan. 2008.
7. Liu, B. and Y. Zhao, "Compact tri-band bandpass filter for WLAN and WiMAX using tri-section stepped-impedance resonators," *Progress In Electromagnetics Research Letters*, Vol. 45, 39–44, 2014.
8. Ghatak, R., M. Pal, P. Sarkar, A.-K. Aditya, and D. R. Poddar, "Tri-band bandpass filters using modified tri-section stepped impedance resonator with improved selectivity and wide upper stopband," *IET Microw. Antennas Propag.*, Vol. 7, No. 15, 1187–1193, 2013.
9. Yang, S., B. Wu, C. Zhu, Y. Wang, and C.-H. Liang, "Compact and high selectivity tri-band bandpass filter using multipath-embedded resonators," *Progress In Electromagnetics Research Letters*, Vol. 50, 35–40, 2014.
10. Liu, S.-K. and F.-Z. Zheng, "A new compact tri-band bandpass filter using step impedance resonators with open stubs," *Journal of Electromagnetic Waves and Applications*, Vol. 26, No. 1, 130–139, 2012.
11. Xu, J., W. Wu, and C. Miao, "Compact microstrip dual-/tri-/quad-band bandpass filter using open stubs loaded shorted stepped-impedance resonator," *IEEE Trans. Microw. Theory and Tech.*, Vol. 61, No. 9, 3187–3199, Sep. 2013.
12. Wei, X.-B., P. Wang, P. Gao, Z.-Q. Xu, J.-X. Liao, L. Jin, and Y. Shi, "Compact tri-band bandpass filter using open stub loaded tri-section $\lambda/4$ stepped impedance resonator," *IEEE Microw. Wireless Compon. Lett.*, Vol. 24, No. 8, 512–514, Aug. 2014.
13. Li, J., S. S. Huang, and J. Z. Zhao, "Design of a compact and high selectivity tri-band bandpass filter using asymmetric stepped-impedance resonators (SIRs)," *Progress In Electromagnetics Research Letters*, Vol. 44, 81–86, 2014.
14. Chen, W.-Y., M.-H. Weng, S.-J. Chang, H. Kuan, and Y.-H. Su, "A new tri-band bandpass filter for GSM, WiMAX and ultra-wideband responses by using asymmetric stepped impedance resonators," *Progress In Electromagnetics Research*, Vol. 124, 365–381, 2012.
15. Luo, S., L. Zhu, and S. Sun, "Compact dual-mode triple-band bandpass filters using three pairs of degenerate modes in a ring resonator," *IEEE Trans. Microw. Theory and Tech.*, Vol. 59, No. 5, 1222–1229, May 2011.
16. Liu, J.-C., F.-S. Huang, C.-P. Kuei, and C.-Y. Liu, "Compact dual-mode double square-loop resonators for WLAN and WiMAX tri-band filter design," *Progress In Electromagnetics Research C*, Vol. 38, 101–113, 2013.
17. Lai, X., C.-H. Liang, H. Di, and B. Wu, "Design of tri-band filter based on stub loaded resonator and DGS resonator," *IEEE Microw. Wireless Compon. Lett.*, Vol. 20, No. 5, 265–267, May 2010.
18. Chen, F.-C. and Q.-X. Chu, "Design of compact tri-band bandpass filter using assembled resonators," *IEEE Trans. Microw. Theory and Tech.*, Vol. 57, No. 1, 165–171, Jan. 2009.
19. Gao, L. and X.-Y. Zhang, "High-selectivity dual-band bandpass filter using a quad-mode resonator with source-load coupling," *IEEE Microw. Wireless Compon. Lett.*, Vol. 23, No. 9, 474–476, Sep. 2013.
20. Hong, J.-S., *Microstrip Filter for RF/Microwave Applications*, 2nd Edition, Chapter 8, Wiley, New York, 2011.
21. Lee, S.-Y. and C.-M. Tsai, "New cross-coupled filter design using improved hairpin resonators," *IEEE Trans. Microw. Theory and Tech.*, Vol. 48, No. 12, 2482–2490, Dec. 2000.